Combined spectroscopic imaging STM and ARPES study of different gaps measured in the cuprate phase diagram

K. Fujita,[1] I. Drozdov,[1] Z. Du,[1] H. Li,[1,2] S.-H. Joo,[1,3,4] J. Lee,[3,4] G. Gu,[1] P. D. Johnson,[1] and T. Valla[1]

[1]*Condensed Matter Physics and Materials Science Department, Brookhaven National Laboratory, Upton, New York 11973, USA*

[2]*Department of Physics and Astronomy, Stony Brook University, Stony Brook, New York 11790, USA*

[3]*Department of Physics and Astronomy, Seoul National University, Seoul 08826, Republic of Korea*

[4]*Center for Correlated Electron Systems, Institute for Basic Science, Seoul 08826, Republic of Korea*

(Received 26 August 2019; revised manuscript received 12 November 2019; published 31 January 2020)

A comparative study of the gaps measured in two techniques, angle-resolved photoelectron spectroscopy and spectroscopic imaging scanning tunneling microscopy, is presented. In particular the study focuses on the more overdoped region of the cuprate phase diagram in the superconducting state. While the total densities of states measured in the two techniques agree very well, it is shown that the peak in the density of states, Δ_{DOS}, is consistently displaced to higher energies relative to the maximal superconducting gap, Δ_0, determined in photoemission. The difference between the two gaps is more evident for the less doped samples reflecting increased normalization of bands. This observation will clearly influence the boundaries in the phase diagrams of the cuprates defined by these two techniques.

DOI: 10.1103/PhysRevB.101.045136

I. INTRODUCTION

High-T_c superconductivity (HTS) remains at the very forefront of condensed matter physics research. Two of the key experimental techniques for investigation of the electronic structure of these materials are represented by angle-resolved photoemission (ARPES) and spectroscopic imaging scanning tunneling microscopy (SI-STM), both of which have undergone an explosion of use following the discovery of HTS. The two techniques complement each other, ARPES being a probe of the electronic structure in momentum space, SI-STM being a probe in real space. They have both contributed much to our understanding of these complex materials. In particular ARPES has demonstrated the d-wave symmetry of the superconducting (SC) gap [1,2] and seemingly the same symmetry for the normal state pseudogap in the underdoped regime [3–5]. Further, ARPES has investigated quasiparticle (QP) self-energies [2,6,7] and, more recently, shown the transition of the Fermi surface (FS) from arcs associated with the uderdoped regime to the full FS characterizing the overdoped regime [8]. SI-STM has also contributed to our knowledge of both the superconducting gap and the normal state pseudogap. With the refinement of the quasiparticle interference (QPI) [9–11] analysis, SI-STM has investigated the FS reconstruction [12]. However, being a more local probe, SI-STM has contributed greatly to our understanding of charge ordering in the cuprates [13,14].

The same information about the underlying electronic structure of a given material is encoded in the measurements from both techniques, ARPES and SI-STM, and ideally they should provide identical information, albeit via different "scattering" routes. Complexity is added to the comparison via the different length scales and different matrix elements associated with the two techniques. SI-STM clearly measures at the nanoscale and has consistently identified local inhomogeneities in the electronic structure in all strongly correlated systems measured. ARPES as a technique is slowly pushing into the nanoscale capability but is not even close to the resolution required to observe inhomogeneities at the level seen in SI-STM measurements. Therefore ARPES sees the spatially averaged picture and we may ask, how does the different spatial sensitivity inhibit or influence comparisons between the two techniques?

As indicated in Fig. 1(a), in ARPES an electron is excited from the sample via interaction associated with the incoming photon and detected at some remote point by the electron spectrometer. In SI-STM on the other hand, an electron tunnels from some point r in the sample to some point r' in the microscope tip or vice versa, as also shown schematically in Fig. 1(a). In ARPES the transition between initial and final electronic state is k conserving and thus momentum information is obtained by measuring the intensity as a function of angle of emission. In SI-STM on the other hand, momentum information is obtained through the technique of QPI analysis which essentially requires nonlocal analysis of standing waves originating from elastic scattering of electrons on local imperfections in the material, thereby providing information in q space, the coupling of different points in k space. However, both techniques are related through a Fourier transform of each other and determine a spectral function $A(\omega)$ [15] such that for ARPES

$$A(\boldsymbol{k},\omega) = -\frac{1}{\pi}\mathrm{Im}G(\boldsymbol{k},\ \omega) \quad \text{and for STM}$$
$$A\,(\boldsymbol{r},\omega) = -\frac{1}{\pi}\mathrm{Im}G(\boldsymbol{r},\ \omega). \tag{1}$$

While, as noted earlier, there has been considerable referencing of information between the two techniques, there have been few studies where they have been directly applied to the

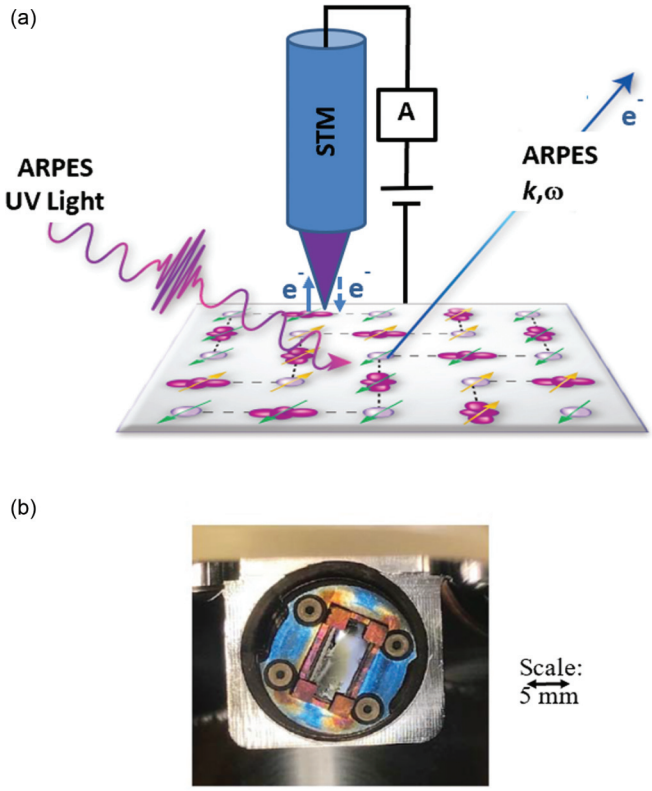

FIG. 1. (a) Schematic of the ARPES process involving the photoexcitation of electrons and the subsequent detection of the latter in free space and schematic of the SI-STM process involving the application of an electric field between a scanning tip and the surface under investigation enabling the tunneling of electrons back and forth between the tip and the surface. We indicate the amplifier (a) in the STM circuit. (b) The sample mounting required to enable the growth and modification of the surface in the MBE system and transfer of the latter to either the ARPES facility or the SI-STM facility. The scale is indicated.

same sample; this because in the past they have inevitably resulted from studies carried out in different experimental systems. The recent development of new facilities, such as the OASIS facility at Brookhaven National Laboratory, which combines *in situ* growth with SI-STM and ARPES, is allowing us to make direct comparisons of their respective information on identical samples. How should we compare the information obtained in the two spectroscopies when one technique SI-STM consistently points to nanoscale inhomogenities and the other technique averages over such phenomena? Indeed, an earlier study has been made to examine the possible role of inhomogeneities and their influence on the ARPES spectra in the antinodal direction [16]. However, in the present study we are in a position to make a more direct comparison of the techniques. We make the comparison at two different points of the phase diagram, one corresponding to near optimal doping and the other in the more highly overdoped regime. In particular, we compare the spectrum $A(\pi, k_F)$ measured in ARPES at the FS crossing in the antinodal direction with the total density of states (DOS) measured in ARPES and the DOS measured in SI-STM. The DOS in ARPES is obtained by integrating the spectral function over momentum space and that in SI-STM by integrating over real space:

$$\mathrm{DOS}(\omega) = \int_k A(\boldsymbol{k}, \omega) dk = \int_r A(\boldsymbol{r}, \omega) dr. \quad (2)$$

This is an important exercise because cuprate phase diagrams are regularly generated as a compilation of data extracted from the two techniques under consideration here and from other techniques and quite often involve studies of different materials, with ill-defined doping levels. Here, we reexamine these issues by performing SI-STM and ARPES experiments on samples with the doping level determined by ARPES.

II. EXPERIMENTAL APPROACH

The experiments within this study were carried out in the new OASIS system which, as already noted, integrates oxide-molecular beam epitaxy (MBE) with ARPES and STM spectroscopic capabilities in a common vacuum system, thereby allowing detailed studies of previously inaccessible materials [17]. Initial samples were slightly overdoped (T_c = 91 K) single crystals of $Bi_2Sr_2CaCu_2O_{8+}$, synthesized by the traveling-solvent floating zone method. To achieve overdoping, the cleaved as-grown samples were transferred to the OASIS MBE chamber (base pressure of 8×10^{-8} Pa) where they were annealed in 3×10^{-3} Pa of cryogenically distilled O_3 at 350−480 °C for ≈1 h. The samples were subsequently cooled to room temperature in the ozone atmosphere and transferred to the ARPES chamber (base pressure of 8×10^{-9} Pa) for analysis using the sample mounting shown in Fig. 1(b). Annealing of as grown crystals in O_3 results in increased doping in the near-surface region, as evidenced by the increased hole FS, reduced spectral gap, and associated transition temperature, T_c. Most of the crystal's bulk volume remained near optimal doping following the ozone annealing. The thickness of the overdoped surface layer was in the sub-μm range, as only the thinnest, semitransparent recleaved flakes showed a significant reduction in T_c in susceptibility measurements.

ARPES measurements were carried out using a Scienta SES-R4000 electron spectrometer with a monochromatized HeI (21.22 eV) radiation source (vacuum ultraviolet-5k). The total instrumental energy resolution was ∼5 meV. The angular resolution was better than ∼0.15° and 0.4° along and perpendicular to the entrance slit of the analyzer, respectively. Following the ARPES studies, the samples can be transferred into the STM facility where measurements are carried out at 7 K. In the latter system topographic images are recorded simultaneously with the tunneling current and with the differential conductance at 1 pA/mV tip-sample junction configuration. Standard lock-in techniques are used for the differential conductance measurements at ν = 895 Hz.

III. RESULTS AND DISCUSSION

Figure 2 shows the spectral intensities measured from the OD91 (T_c = 91 K) material in the two spectroscopies, SI-STM on the left and ARPES on the right. The SI-STM measurements were made over an area of 25 × 25 nm. The inset in Fig. 2(b) shows the associated distribution of peak positions in local DOS, with a mean distribution of Δ_{DOS} = 37 meV giving a mean field value of $2\Delta_{\mathrm{DOS}}/kT_c = 9.4$.

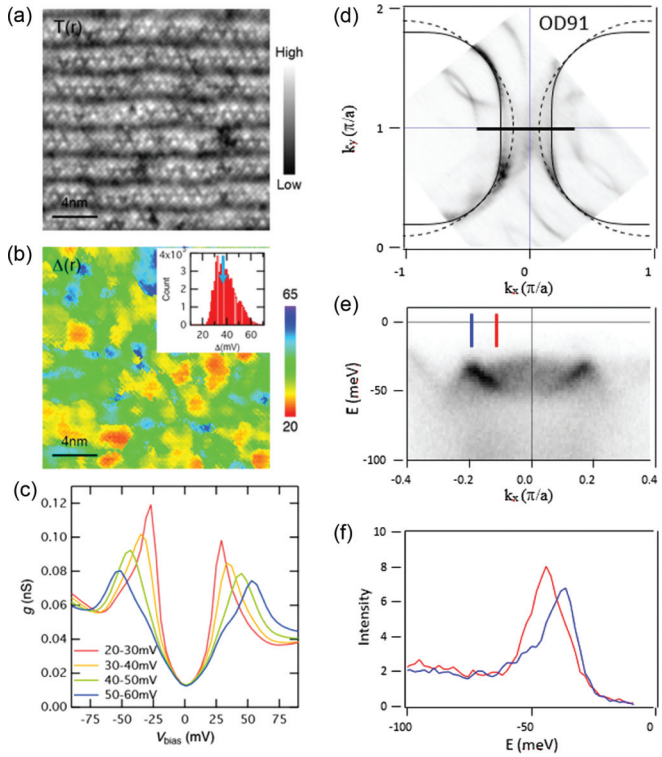

FIG. 2. (a) Topography and (b) gap map measured from the OD91 ($T_c = 91$ K) sample over an area 25×25 nm area using SI-STM. The inset shows the distribution of different gap sizes measured in the sampling area. The blue arrow indicates the peak energy determined in the DOS measurement from both techniques. (c) Gap-sorted averaged dI/dV spectra from SI-STM. (d) ARPES measured constant energy surface corresponding to 15 meV below the chemical potential along with tight binding fits, indicated by the solid and dashed lines. (e) Shows a cut in the antinodal region in the direction indicated by the solid line in (d). (f) Shows two EDC cuts indicated in (e) by the blue and red lines.

Several SI-STM dI/dV spectra extracted from different places in the gap map are also shown. Figure 2(d) shows the ARPES intensity measured in the superconducting state ($T = 20$ K) at 15.0 meV binding energy, along with tight binding fits for the bonding and the antibonding state, indicated by the solid and dashed lines, respectively. From the FS area, obtained as the contours connecting the momentum points at minimal gap loci, the doping level can be directly extracted: $p = 0.20 \pm 0.01$ in the present case [18,19]. Figure 2(e) shows the dispersion of the electronic states along the momentum cut in the antinodal region indicated by the solid line in Fig. 2(d). The bottom panel shows the two energy distribution curves (EDC) taken at two momenta indicated in Fig. 2(e). The blue spectrum, corresponding to the Fermi momentum k_F, provides a true measure of the maximum gap, $\Delta_0 = 34$ meV. The red EDC, recorded away from k_F and closer to the $(\pi, 0)$ point, provides an indication of the state's renormalized dispersion that is expected to contribute significantly to the density of states and shift its peak away from Δ_0 [19,20].

In Fig. 3(a) we compare the total DOS measured in SI-STM with that measured in ARPES for the as grown OD91 material. In Fig. 3(b) we show the same for the OD50 material. Noted earlier, in STM the DOS is determined by integrating the spectra in real space, in ARPES by integrating in momentum space, in accordance with Eq. (2). We note that the DOS at a given energy DOS(E) is given by

$$\mathrm{DOS}(E) = \int dS \frac{1}{|\nabla_k E|}, \tag{3}$$

which will clearly be dominated by regions of the electronic structure where the dispersion is less. Thus a particular band's contribution will increase with increasing renormalization.

We note in Fig. 3, excellent agreement between the DOS measured in the two techniques, despite the fact that the matrix element effects and the sampling depths are different. The DOS shown in Figs. 3(a) and 3(b) are dominated by the V-shaped gap straddling the chemical potential, reflecting the d-wave order parameter in the superconducting state. Also shown in each figure is the ARPES spectrum measured exactly at the FS crossing, (π, k_F). In this case the k_F is determined by using EDC analysis to track the dispersion of the Bogolubov dispersion in the superconducting state.

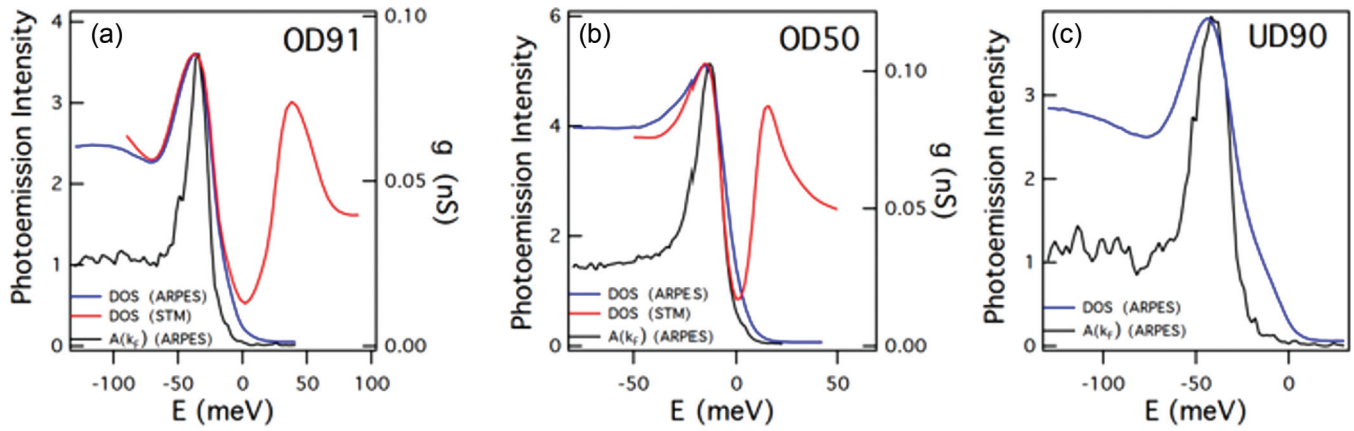

FIG. 3. (a) Comparison of the integrated DOS measured in SI-STM (red curve) and the integrated DOS measured in ARPES (blue curve) from the OD91 sample. Also shown is the ARPES spectrum, $A(k, \omega)$, measured exactly at (π, k_F). (b) The same as in (a) but now for the OD50 sample. (c) Comparison of the integrated DOS measured in ARPES from the slightly underdoped UD85 sample with the ARPES spectrum, $A(k, \omega)$, measured exactly at (π, k_F).

This provides an accurate measurement of Δ_0, the true maximum gap of the momentum dependent superconducting gap, $\Delta(k) = \Delta_0(\cos k_x - \cos k_y)$. It is clear that, while the DOS measured by the two techniques appears nearly identical, its peak is consistently shifted to higher binding energy relative to the true Δ_0 measured at the FS. For the two doping levels studied here, the DOS peak is at 37 and 15.5 meV, while the corresponding Δ_0 is 34 and 14 meV for the OD91 and OD50 samples, respectively. The blue arrow in the inset of Fig. 2(b) compares the peak value of the DOS determined in the two techniques with the distribution of gaps determined in the spatially resolved STM studies. A value of $\Delta_0 = 34$ meV for the OD91 sample is nearly identical to value of 35 meV found in optical conductivity studies of the same material [21]. We note that a more refined analysis may be applied to determine the maximal gap more accurately, namely the tomographic density of states method [22]. This will take account of the contributions from the Fermi-Dirac occupation and overall experimental energy resolution. We anticipate that this will shift Δ_0 to lower energies, thereby increasing the discrepancy between the DOS and Δ_0.

We note that in the noninteracting case, the DOS peak should occur exactly at Δ_0 for a d-wave gap. As the DOS peak position is particle-hole symmetric, we can exclude the influence of the van Hove singularity (VHS) on its position. At these doping levels, the VHS is present only on the occupied part of the spectrum, for both bonding and antibonding states. Therefore, the broadening and shifting of the DOS peak to the high binding energy side likely reflects a strong renormalization of the Bogoliubov quasiparticles on some bosonic mode, as indicated in Fig. 2(e) [7,19,20]. With reference to Eq. (3), strongly renormalized, massive states dispersing within the mode energy have higher DOS than strongly dispersing bands outside this range. The result is the shift of the DOS peak away from the noninteracting position at Δ_0, on both the particle and hole sides of the spectrum.

In constructing the phase diagrams of the cuprate superconductors, the gaps from ARPES and STM are often plotted on the same scale as being equivalent quantities. We have shown here that the peak positions in the DOS in either STM or ARPES generally do not correspond to the true gap Δ_0, measured at the FS in ARPES. The differences may not be large, especially on the overdoped side, where the renormalizations get weaker, but they will affect some characteristic boundaries defined in the phase diagrams, particularly in the underdoped region where we may anticipate larger renormalizations and further, the pseudogap making a contribution. We illustrate this in Fig. 3(c), where, recognizing that the DOS in the two techniques under consideration is identical, we simply present a comparison of the ARPES determined DOS with the ARPES $A(\pi, k_F)$ for the slightly underdoped sample, $T_c = 85$ K, achieved by annealing in the ARPES chamber for several hours [18]. Now the difference in the two gaps has increased to 5 meV.

There is also another interesting observation regarding the SI-STM and ARPES data. The gap maps and dI/dV curves in the SI-STM studies would suggest a relatively inhomogeneous system as evidenced by the wide range of gaps in the local DOS [Figs. 2(b) and 2(c)]. The ARPES studies, on the other hand, with well-defined FSs and a Luttinger count, based on fitting to the FS, suggest a homogeneous system with well-defined doping level ($\Delta p < \pm 0.01$ near optimal doping) [18], closer to the level of inhomogeneities in p inferred from the bulk sensitive heat capacity measurements [23]. We note that the present studies are all carried out in the superconducting state where the coherence associated with the latter renders less sensitivity to local disorder. Indeed the SI-STM maps look much more homogeneous at low energies, inside the superconducting gap, implying a more uniform Δ_0 and p. Interestingly, a similar dichotomy between local and nonlocal phenomena has been reported elsewhere in studies of another strongly correlated systems, Sr_2IrO_4, [24] and more recently in twisted bilayer graphene where a range of local twist angles do not appear to influence nonlocal transport measurements [25]. To examine these issues, further experimental and theoretical studies will be needed, including a careful re-evaluation of basic principles of the two techniques under discussion here.

In summary we have confirmed the relationship between the DOS measured in ARPES and that measured in SI-STM; this despite the observation that the two techniques seemingly indicate different levels of inhomogeneity. Further, by comparing the gaps determined in these DOS with the gap measured at (π, k_F) we show that the DOS may be an indicator of relative changes but is not a measure of absolute values of Δ_0 and the two quantities should not be interchangeably used in the development of phase diagrams.

ACKNOWLEDGMENTS

The authors acknowledge useful discussions with J. Tranquada and I. Božović. The work at Brookhaven National Laboratory is funded by the U.S. Department of Energy, Office of Basic Energy Sciences, under Contract No. DE-SC0012704.

[1] Z.-X. Shen, D. S. Dessau, B. O. Wells, D. M. King, W. E. Spicer, A. J. Arko, D. Marshall, L. W. Lombardo, A. Kapitulnik, and P. Dickinson *et al.*, Phys. Rev. Lett. **70**, 1553 (1993).

[2] A. Damascelli, Z. Hussain, and Z.-X. Shen, Rev. Mod. Phys. **75**, 473 (2003).

[3] H. Ding, T. Yokoya, J. C. Campuzano, T. Takahashi, M. Randeria, M. R. Norman, T. Mochiku, K. Kadowaki, and J. Giapintzakis, Nature (London) **382**, 51 (1996).

[4] D. S. Marshall, D. S. Dessau, A. G. Loeser, C.-H. Park, A. Y. Matsuura, J. N. Eckstein, I. Bozovic, P. Fournier, A. Kapitulnik, W. E. Spicer *et al.*, Phys. Rev. Lett. **76**, 4841 (1996).

[5] C. Renner, B. Revaz, J.-Y. Genoud, K. Kadowaki, and Ø. Fischer, Phys. Rev. Lett. **80**, 149 (1998).

[6] T. Valla, A. V. Fedorov, P. D. Johnson, B. O. Wells, S. L. Hulbert, Q. Li, G. D. Gu, and N. Koshizuka, Science **285**, 2110 (1999).

[7] P. D. Johnson, T. Valla, A. Fedorov, Z. Yusof, B. O. Wells, Q. Li, A. R. Moodenbaugh, G. D. Gu, N. Koshizuka, C. Kendziora *et al.*, Phys. Rev. Lett. **87**, 177007 (2001).

[8] H.-B. Yang, J. D. Rameau, Z.-H. Pan, G. D. Gu, P. D. Johnson, H. Claus, D. G. Hinks, and T. E. Kidd, Phys. Rev. Lett. **107**, 047003 (2011).

[9] J. E. Hoffman, K. McElroy, D.-H. Lee, K. M. Lang, H. Eisaki, S. Uchida, and J. C. Davis, Science **297**, 1148 (2002).

[10] K. McElroy, R. W. Simmonds, J. E. Hoffman, D.-H. Lee, J. Orenstein, H. Eisaki, S. Uchida, and J. C. Davis, Nature (London) **422**, 592 (2003).

[11] Q.-H. Wang and D.-H. Lee, Phys Rev. B **67**, 020511(R) (2003).

[12] K. Fujita, C. K. Kim, I. Lee, J. Lee, M. H. Hamidian, I. A. Firmo, S. Mukhopadhyay, H. Eisaki, S. Uchida, M. J. Lawler *et al.*, Science **344**, 612 (2014).

[13] J. E. Hoffman, E. W. Hudson, K. M. Lang, V. Madhavan, H. Eisaki, S. Uchida, and J. C. Davis, Science **295**, 466 (2002).

[14] Y. Kohsaka, C. Taylor, K. Fujita, A. Schmidt, C. Lupien, T. Hanaguri, M. Azuma, M. Takano, H. Eisaki, H. Takagi, S. Uchida, and J. C. Davis, Science **315**, 1380 (2007).

[15] P. Abbamonte, E. Demler, J. C. Davis, and J. C. Campuzano, Physica C **481**, 15 (2012).

[16] N. Zaki, H.-B. Yang, J. D. Rameau, P. D. Johnson, H. Claus, and D. G. Hinks, Phys. Rev. B **96**, 195163 (2017).

[17] C.-K. Kim, I. K. Drozdov, K. Fujita, J. C. Séamus Davis, I. Božović, and T. Valla, J. Elect. Spect. Relat. Phenom. (2018), doi: 10.1016/j.elspec.2018.07.003.

[18] I. K. Drozdov, I. Pletikosić, C.-K. Kim, K. Fujita, G. D. Gu, J. C. Séamus Davis, P. D. Johnson, I. Božović, and T. Valla, Nat. Commun. **9**, 5210 (2018).

[19] T. Valla, I. K. Drozdov, and G. D. Gu, Nat. Commun. (2020), doi: 10.1038/S41467-020-14282-4.

[20] H. Li, X. Zhou, S. Parham, T. J. Reber, H. Berger, G. B. Arnold, and D. S. Dessau, Nat. Commun. **9**, 1 (2018).

[21] C. C. Homes, J. J. Tu, J. Li, G. D. Gu, and A. Akrap, Sci. Rep. **3**, 3446 (2013).

[22] T. J. Reber, N. C. Plumb, Z. Sun, Y. Cao, Q. Wang, K. McElroy, H. Iwasawa, M. Arita, J. S. Wen, Z. J. Xu *et al.*, Nat. Phys. **8**, 606 (2012).

[23] J. W. Loram, J. L. Tallon, and W. Y. Liang, Phys. Rev. B **69**, 060502(R) (2004).

[24] Y. K. Kim, N. H. Sung, J. D. Denlinger, and B. J. Kim, Nat. Phys. **12**, 37 (2016).

[25] A. Uri, S. Grover, Y. Cao, J. A. Crosse, K. Bagani, D. Rodan-Legrain, Y. Myasoedov, K. Watanabe, T. Taniguchi, P. Moon *et al.*, arXiv:1908.04595 [cond-mat.mes-hall].